Theoretical Verification of the Infinite Constant Power Speed Range of the Brushless DC Motor Driven by Dual Mode Inverter Control*

J. S. Lawler
The University of Tennessee
Knoxville, Tennessee

J. M. Bailey and John W. McKeever
The Oak Ridge National Laboratory
Oak Ridge, Tennessee

Abstract

The differential equations that describe the operation of the brushless dc motor (BDCM) driven by dual mode inverter control (DMIC) are solved analytically. Explicit expressions for peak and rms motor current and average motor power are derived. The analysis is performed neglecting all motor loss mechanisms. The results provide a theoretical verification that the constant power speed range (CPSR) of the BDCM is infinite when driven by the DMIC. While speed sensitive motor losses limit the CPSR of any practical drive to a finite value, there is no inherent limitation imposed by the DMIC. The analytic formulas provide useful drive design guidance without requiring simulation or laboratory experimentation.

1. Introduction

In previous work the authors have used simulation and laboratory testing to show that the constant power speed range (CPSR) of the brushless dc motor (BDCM) is 6:1 or greater when the BDCM is driven by the dual mode inverter control (DMIC) [1,2]. The DMIC is a novel inverter topology and semiconductor firing scheme that has been developed to provide the wide CPSR required for electric vehicle applications for BDCMs having low internal inductance [3]. In this work, the differential equations describing the BDCM when driven by the DMIC are solved to provide analytical expressions for the instantaneous motor phase currents, the peak and rms motor current, and for the average power developed by the BDCM when driven by the DMIC. The analysis is done with all motor loss mechanisms neglected and confirms that there are no inherent limitations to the CPSR when the BDCM is driven by the DMIC. Specifically, the motor current remains within the rated value at high speed while rated power is produced and the CPSR is theoretically infinite. In a practical drive the speed sensitive motor losses will limit the CPSR to a finite value. The analysis presented provides useful guidance in determining motor performance, especially dependence on motor inductance and dc supply voltage, without time domain simulation or experimentation.

The remainder of the paper includes four sections. The second section reviews the DMIC inverter topology and semiconductor-firing scheme. Section 3 contains the BDCM model used in the analysis and provides the parameters of an example motor that has been designed and built for operation with the DMIC. Section 4 contains the analytical solution to the relevant differential equations for transistor dwell angles of 120 and 180°. The analysis shows that either dwell angle results in an infinite CPSR. However, the 180° dwell case results in substantially more power with essentially the same magnitude motor current. The final section contains our conclusions.

2. DMIC Inverter Topology and Semiconductor Firing Scheme

The DMIC inverter topology and permanent magnet motor model used in this work are shown in Fig. 1. The inverter consists of a common six-transistor voltage fed inverter (VFI) bridge, each transistor having an anti-parallel bypass diode which is interfaced to the motor through an ac voltage controller. The ac voltage controller consists of three pairs of anti-parallel SCRs. A detailed discussion of the operation of the inverter is given in [4] and only a brief discussion is given here.

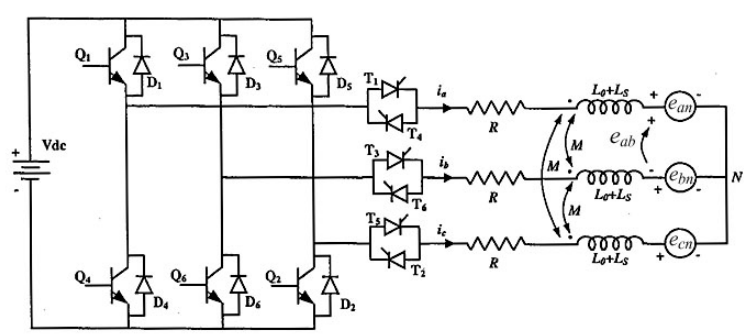

Fig. 1. DMIC inverter topology and permanent magnet motor model.

• Prepared by the Oak Ridge National Laboratory, managed by UT-Battelle, LLC, for the U.S. Department of Energy under contract DE-AC05-00OR22725.
The submitted manuscript has been authored by a contractor of the U.S. Government under contract DE-AC05-00OR22725. Accordingly, the U.S. Government retains a nonexclusive, royalty-free license to publish or reproduce the published form of this contribution, or allow others to do so, for U.S. Government purposes.

The purpose of the thyristors is to block undesired conduction of the bypass diodes during high-speed operation. During high speed motoring the magnitude of the motor emf is substantially larger than the value of the dc supply voltage. Since the bypass diodes form a diode rectifier between the high voltage source of the motor emf and the dc supply there is a natural tendency towards regeneration when the common VFI is used. In the DMIC inverter motor current flows through the series combination of a transistor and a thyristor. Since the thyristor will not reverse conduct, the current is shut off at the current zero crossing. In previous work [4,5] it was shown that when conventional phase advance [6] is applied using the common VFI that the high-speed operation is a mixture of motoring and regeneration. For low inductance motors, the current magnitude at high speed with conventional phase advance may be several times greater than rated and the mixture of motoring and regeneration is extreme. The regeneration is associated with the conduction of the bypass diodes while the motoring component is associated with the conduction of the transistors. The braking component is large and cancels a like portion of the motoring component leaving a modest net motoring component. In the DMIC, the thyristors, which will not reverse conduct, eliminate the braking component that would otherwise result from bypass diode conduction [1,4]. The elimination of the braking component allows rated power to be developed at a greatly reduced current level. Despite the additional semiconductor drops associated with the thyristors, the efficiency of the DMIC drive is superior to that of conventional phase advance when the motor inductance is low. In addition to keeping the motor current within rating during high-speed operation at rated power, the thyristors provide several fault tolerance benefits. The thyristors make it possible to extinguish motor current within one half electrical cycle following a fault in the dc supply system or in the transistor inverter. This would be done by simply inhibiting further firing of the thyristors which then shut off at their first current zero crossing. The thyristors also preclude uncontrolled regeneration following loss of firing signals caused by a controller board failure. In addition, the thyristors block the voltage levels associated with motor emf, which may be several time larger than the dc supply voltage, while the transistors block only the supply voltage. This feature can protect the low voltage transistors from motor emf voltage levels in the event of loss of the dc bus during high-speed operation.

The firing scheme of the DMIC controller for high-speed motoring operation is shown in Fig. 2. As with the conventional phase advance method [6], the transistors are fired at an advance angle, θ_a, but the advance angle is defined relative to the intersection of one of the phase-to-phase back emfs with the dc supply voltage. Figure 2 shows the firing scheme for the transistors and thyristors of phase a referred to the line-to-line emf, e_{ab}. The firing of the semiconductors in phase b would be completely analogous to Fig. 2 with the relevant line-to-line emf being e_{bc}, and firing in phase c would be referred to the voltage e_{ca}. In one fundamental electrical cycle, there are six distinct intervals, which involve one phase being connected to the positive rail of the dc supply and one phase being connected to the negative rail of the supply. Let (c+,b-) denote a connection where phase c is connected to the positive rail of the dc supply while phase b is connected to the negative rail. The various phase combinations are (c+,b-), (a+,b-), (a+,c-), (b+,c-), (b+,a-), and (c+,a-). Each interval lasts for 60 electrical degrees before one of the conducting phases is exchanged for the idling phase. Once a phase is energized, it remains energized for two 60° intervals before being rotated out as the idling phase. At the beginning of each of these intervals is a commutation interval during which the outgoing phase current falls to zero while the incoming phase current rises to operating level.

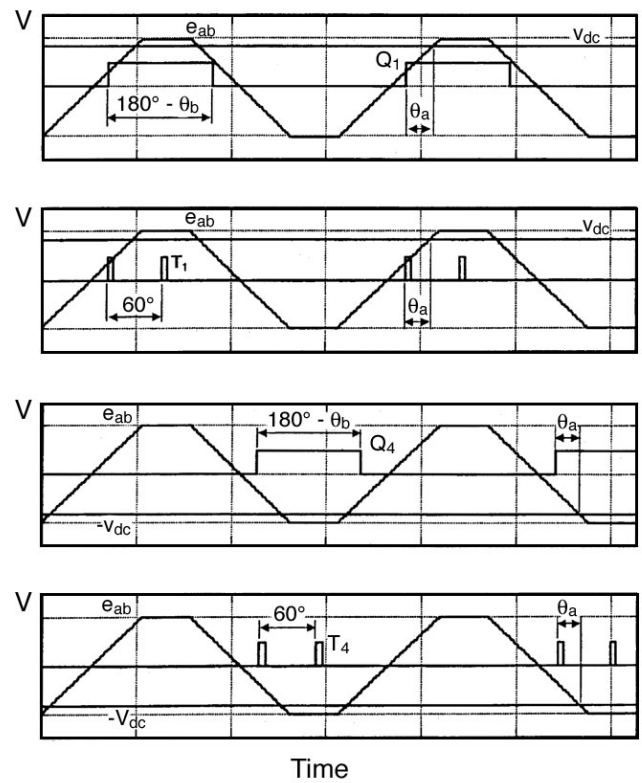

Fig. 2. DMIC firing scheme for phase a semiconductors in high speed motoring mode.

In Fig. 2, the commanded transistor dwell angle, θ_d, is denoted as 180° minus the "blanking angle," θ_b. In a PWM inverter, some interval is set aside between the time that one transistor in a given phase pole is to be turned off and before the companion transistor in that pole is to be turned on. This interval is referred to as the blanking time and it provides a safeguard against inadvertent short circuits of the supply due to variations in the turn off and turn on times of the transistors. There is good reason to reduce the blanking angle from 60° to a value closer to 0°, or equivalently to increase the transistor dwell from 120° towards 180°. At the beginning of a commutation interval, the phase current in the outgoing phase may be large, but decreasing in magnitude due to the emf crossing V_{dc}. That phase is contributing a great deal of power because of simultaneously high current and high voltage. At a blanking angle of 60° (dwell of 120°), the outgoing phase is shut off by turning off its transistor and allowing the phase current to transfer to the bypass diode of the opposite transistor. The thyristor shuts off when the current reaches zero. This sudden reversal of the outgoing phase from one rail of the supply to the opposite rail hastens commutation causing the outgoing phase to go off quickly. However, since the outgoing phase current is already decreasing in magnitude, allowing the outgoing transistor

to stay on longer, by decreasing the blanking angle and thereby increasing the dwell, will slow down the commutation process. Slowing down commutation prolongs the period of simultaneous high current-high voltage in the outgoing phase. As long as the current in the outgoing phase reaches zero within the 60° interval allowed for commutation, the amount of power developed will be increased, and substantially so, at the expense of a slight increase in rms current. The increase in power depends on the motor inductance and may approach 50% of rating, while the increase in rms current is small. Care must be taken not to run the blanking angle down too far when the motor is operating at speeds that are only slightly greater than base speed. In such cases the back emf is only marginally larger in magnitude than V_{dc}, and the outgoing phase may not commutate at all. We have found that the blanking angle should be set at 60° at base speed and reduced gradually to about 10° at 1.5 to 2.0 times base speed. Equivalently, the commanded transistor dwell angle is increased from 120° at base speed to a value of 170° at 1.5-2.0 times base speed. This avoids commutation failures and results in the highest possible power production at high speed.

The transition from below base speed operation to above base speed is a mixture of phase advance and conventional hysteresis band current regulation, involving adjustment of the advance angle, θ_a, and the dwell angle, θ_d, as well as the set-point of the phase current regulator. Smooth adjustment by the transition control is important in electric vehicle applications so that the operator experiences smooth changes in vehicle speed near the base speed of the motor. A transition control, implemented in a digital signal processor, has been developed and the results of laboratory testing will be reported in the future. In this work we focus exclusively on motoring operation at speeds of two or more times base speed.

The next section contains the motor model and the parameters of an example motor used for illustration.

3. Motor Model and Example Motor Parameters

The following notation describes parameters of the BDCM:

p = number of poles
N_b = base speed in rpm
E_b = phase-to-neutral back emf at base speed
L_o = leakage inductance per phase
L_s = self inductance per phase
M = mutual inductance per phase
L = equivalent inductance per phase
$= L_o + L_s + M$
R = winding resistance per phase
V_{an} = applied phase a-to-neutral voltage
V_{ab} = applied phase a-to-phase b voltage
e_{an} = phase a-to neutral back emf
e_{ab} = phase a-to-phase b back emf
N = actual rotor speed in rpm
n = relative speed = N/N_b
$E(n)$ = peak phase-to-neutral back emf at speed $n = nE_b$
Ω_b = base speed in electrical rad/sec = $\frac{p}{2}\frac{2\pi N_b}{60}$

With surface mounted magnets the motor is modeled by the phase equations [7]

$$\begin{bmatrix} v_{an} \\ v_{bn} \\ v_{cn} \end{bmatrix} = \begin{bmatrix} L_o + L_s & -M & -M \\ -M & L_o + L_s & -M \\ -M & -M & L_o + L_s \end{bmatrix} \frac{d}{dt} \begin{bmatrix} i_a \\ i_b \\ i_c \end{bmatrix} + \begin{bmatrix} R & 0 & 0 \\ 0 & R & 0 \\ 0 & 0 & R \end{bmatrix} \begin{bmatrix} i_a \\ i_b \\ i_c \end{bmatrix} + \begin{bmatrix} e_{an} \\ e_{bn} \\ e_{cn} \end{bmatrix} . \quad (1)$$

The phase-to-neutral back emfs are trapezoids with 120 º of flat top in each half cycle and with amplitude that is linear in speed. The phase b and c emfs are delayed from the phase a emf by one third and two thirds of a cycle respectively.

Since the phase currents sum to zero, only two of these equations are independent and a second order state model can be derived. Preserving phase a and c currents results in:

$$\frac{d}{dt}\begin{bmatrix} i_a \\ i_c \end{bmatrix} = \frac{-R}{L}\begin{bmatrix} i_a \\ i_c \end{bmatrix} + \frac{1}{3L}\begin{bmatrix} 2 & -1 \\ -1 & 2 \end{bmatrix}\begin{bmatrix} v_{ab} - e_{ab} \\ v_{cb} - e_{cb} \end{bmatrix} . \quad (2)$$

The Eq. (2) model can be further simplified when only two phases are conducting. Assuming that phase c is off, then the current in phase b is the negative of the current in phase a and the model simplifies to:

$$\frac{d}{dt} i_a = \frac{-R}{L} i_a + \frac{1}{2L}\left[v_{ab} - e_{ab}\right] . \quad (3)$$

At the instants that switching occurs there is a finite commutation interval during which the outgoing phase current goes to zero. During this short commutation interval all three phases are conducting and the appropriate model is that in Eq. (2). Once the commutation is complete only two phases are conducting and the model in Eq. (3) can be used.

The example motor has been designed and built by the Oak Ridge National Laboratory especially for operation with the DMIC. The parameters of the example motor are:

N_b = base speed = 1000 rpm
p = 18 poles
L = 158 μH per phase
R = 0.026 ohms
E_b = peak phase-to-neutral back emf at base speed . (4)
= 46.96 volts
P_r = rated power = 20,092 watts (26.9 horsepower)
T_r = rated torque = 191.9 Nm
V_{dc} = dc supply voltage = 130 volts

The 130 volts dc supply allows the motor to develop rated power at base speed without phase advance.

Assuming the classical idealized rectangular phase current wave shape of the BDCM (rectangular shape of 120° duration each half cycle), the theoretical peak and rms currents of this motor are:

$$I_{pk} = \text{peak current} = \frac{P_r}{2E_b} = 213.9 \text{ amps}$$
$$I_{rms} = \text{rms current} = I_{pk}\sqrt{\frac{2}{3}} = 174.7 \text{ amps} \quad . \tag{5}$$

These values will be used as ratings in the remainder of the discussion.

Figure 3 provides graphical insight into the impact of transistor dwell angle on the performance of the DMIC in

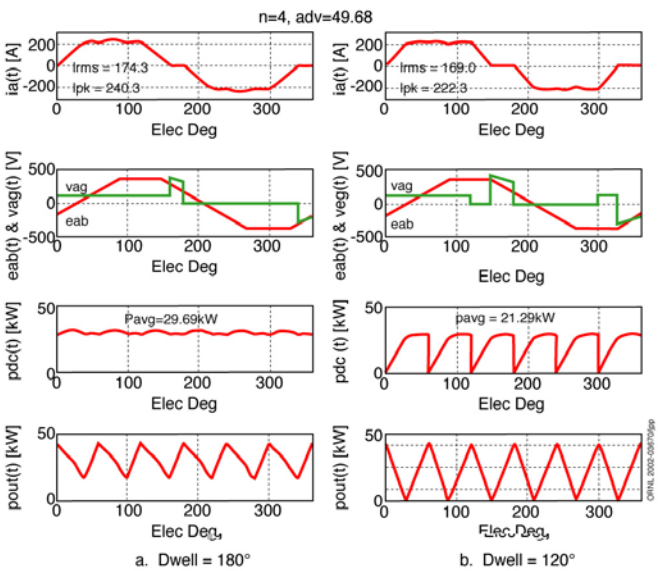

Fig. 3. Impact of dwell angle on DMIC performance.

driving the BDCM at high speed. The plots were generated with a detailed simulator of the motor with the inverter and switching logic of the DMIC. The simulation was done with all semiconductors represented by ideal switches and the motor resistance was neglected. The figure shows the simulated performance at relative speed of 4 and an advance angle of 49.68 degrees. This advance angle was chosen since it corresponds to rated rms current when the dwell angle is 180°. Plots of instantaneous phase a current, phase a to ground voltage (negative rail of the dc supply), the line-to-line emf between phase a and b, the instantaneous power from the dc supply and the total instantaneous power developed by the motor are given in Fig. 3. The figure shows the results for transistor dwell angles of 180° and 120°. The following observations are based on the figure:

- The current waveforms differ primarily in the commutation time. The current decreases to zero faster with 120° dwell than with 180°. The rms and peak current values with 120° dwell (169.0 amp, 222.3 amp) are slightly smaller than the values corresponding to 180° (174.3 amp, 240.3 amp).
- There is a dramatic difference in the average power developed by the motor. For the 180° dwell case the average power is 29.69 kW while 21.29 kW is developed with the dwell set at 120°. The power developed at base speed, without phase advance is 20.1 kW. Thus, there is an increase of almost 48% of rated power when operating at high speed with 180° dwell.
- The instantaneous supply power and the instantaneous power output of the motor have different wave shapes but have the same average value. The difference in wave shape is due to the energy storage associated with the motor inductance.
- Although not shown in the figure, the dc link current has the same wave shape as the instantaneous supply power. For the 120° dwell case, the dc current drops to zero at the beginning of each commutation interval. The incoming phase current is initially zero and the outgoing phase is transferred from the dc supply to a circulating path through a bypass diode. For the 180° dwell case the outgoing phase is left connected to the dc supply and the dc link current is much smoother.

In the next section the differential equations describing the BDCM driven by the DMIC are solved for the instantaneous motor phase currents. Because of the symmetry of operation, the solution during a single 60° interval is sufficient to completely characterize the motor behavior over a full cycle.

4. Analytical Solution for the BDCM Phase Currents

In this section we show that when the motor loss mechanisms are neglected that the theoretical limit to the CPSR using the DMIC is infinite. The loss factors such as friction and windage, hysteresis and eddy current losses, and semiconductor switching losses may place a practical limit on the CPSR but the control has no inherent limiting consideration that would cause the power to eventually begin decreasing with speed.

With the change of variable,

$$\theta = n\,\Omega_b\,t\,, \tag{6}$$

the state model when all three phases are conducting, Eq. (2), becomes

$$\frac{d}{d\theta}\begin{bmatrix} i_a \\ i_b \end{bmatrix} = \frac{-R}{n\,\Omega_b\,L}\begin{bmatrix} i_a \\ i_b \end{bmatrix} + \frac{1}{3\,n\,\Omega_b\,L}\begin{bmatrix} 2 & -1 \\ -1 & 2 \end{bmatrix}\begin{bmatrix} v_{ab} - e_{ab} \\ v_{cb} - e_{cb} \end{bmatrix}\,, \tag{7}$$

while the model representing periods when only two phases are conducting, Eq. (3), becomes

$$\frac{d}{d\theta} i_a = \frac{-R}{n\,\Omega_b\,L}\,i_a + \frac{1}{2\,n\,\Omega_b\,L}\left[v_{ab} - e_{ab}\right]\,. \tag{8}$$

Consider the transition from the phase pair (c+,b-) to the phase pair (a+,b-), i.e. c is the outgoing phase and a is the incoming phase. The pair (c+,b-) denotes c connected to the positive rail of the dc supply and b connected to the negative rail. Let the time reference, $\theta = 0$, correspond to the instant that phase a is to be connected to the positive terminal of the supply. Assuming that the relative speed n is greater than 2 the back emfs can be

analytically described during the 60 degree interval that the operating pair is (a+,b-) by:

$$
\begin{aligned}
e_{ab}(\theta) &= \frac{6nE_b}{\pi}(\theta-\theta_a+\frac{\pi V_{dc}}{6nE_b}) && 0\le\theta\le\pi/3 \\
e_{cb}(\theta) &= \frac{6nE_b}{\pi}(\theta-\theta_a+\frac{\pi V_{dc}}{6nE_b}+\frac{\pi}{3}) && 0\le\theta\le\theta_a-\frac{\pi V_{dc}}{6nE_b} \\
&= 2nE_b && \theta_a-\frac{\pi V_{dc}}{6nE_b}\le\theta\le\pi/3
\end{aligned}
\quad . (9)
$$

These waveforms are shown in Fig. 4. Note that $e_{ab}(\theta_a)\equiv V_{dc}$ consistent with the fact that phase a is to be energized θ_a radians ahead of the intersection of e_{ab} with V_{dc}. To insert phase a positively, we fire transistor Q1 and thyristor T1 engaging the phase a terminal to the positive rail of the dc supply. The treatment of the outgoing phase, phase c, depends on the transistor dwell angle. Dwell angle values of 180° and 120° are treated separately below. The motor phase winding resistance is neglected in both cases. It is assumed that the advance angle is greater than 30° but less than 60 – 30 $V_{dc}/(n\ E_b)$. This range covers most high speed operating conditions when operating near rated rms current.

4.1 Phase Currents with θ_d = 180°

When the commanded transistor dwell is 180°, the outgoing phase, phase c, is left connected to the positive rail of the dc supply by extending the gate command for Q5 beyond 120°. Once the current in phase c decreases to zero, thyristor T5 will shut off precluding further conduction in phase c independent of the command to transistor Q5. Consequently in Eq. (7) set

$$v_{ab} = v_{cb} = +V_{dc}\,. \tag{10}$$

The initial phase currents that put the motor immediately into periodic steady state can be shown to be:

$$
\begin{aligned}
i_a(0) &= 0 \\
i_b(0) &= -\frac{E_b}{\Omega_b L}(2\theta_a-\frac{\pi}{3})\,. \\
i_c(0) &= \frac{E_b}{\Omega_b L}(2\theta_a-\frac{\pi}{3})
\end{aligned}
\tag{11}
$$

It is straightforward to show that the resulting phase currents during the commutation interval are:

$$
\begin{aligned}
i_a(\theta) &= \frac{E_b}{\Omega_b L}\left\{\left[\frac{2\theta_a}{\pi}+\frac{2}{3}\right]\theta-\frac{1}{\pi}\theta^2\right\} \\
i_b(\theta) &= \frac{E_b}{\Omega_b L}\left\{\left[\frac{\pi}{3}-2\theta_a\right]+\left[\frac{2}{3}-\frac{4\theta_a}{\pi}\right]\theta+\frac{2}{\pi}\theta^2\right\} \\
i_c(\theta) &= \frac{E_b}{\Omega_b L}\left\{2\theta_a-\frac{\pi}{3}+\left[\frac{2\theta_a}{\pi}-\frac{4}{3}\right]\theta-\frac{1}{\pi}\theta^2\right\} \\
&\quad 0\le\theta\le\theta_c
\end{aligned}
\quad , \tag{12}
$$

where θ_c is the commutation angle, that is the angle at which the current in the outgoing phase, phase c in this case, reaches zero. Setting $i_c(\theta)$ in Eq. (12) to zero and solving for θ_c yields

$$\theta_c = 2\theta_a-\frac{\pi}{3}\ . \tag{13}$$

The phase currents at the end of the commutation interval are

$$
\begin{aligned}
i_a(\theta_c) &= \frac{E_b}{\Omega_b L}(2\theta_a-\frac{\pi}{3}) \\
i_b(\theta_c) &= -i_a(\theta_c) \\
i_c(\theta_c) &= 0
\end{aligned}
\quad . \tag{14}
$$

In order to maximize power conversion efficiency it is desirable that the gate signal for Q5 remains in the ON condition until commutation is complete. Equation (13) yields the minimum commanded transistor dwell angle to make this occur; that is, set the commanded transistor dwell angle θ_d such that

$$\theta_d \ge \frac{2\pi}{3}+\theta_c = \frac{\pi}{3}+2\,\theta_a\ . \tag{15}$$

After commutation is complete, the motor is running on only phases a and b and the model of Eq. (3) applies. Assuming that the relative speed, n, is two or more, the back emf e_{ab} is described as noted above no matter what the advance angle may be. For smaller n, and a small advance angle, it could happen that e_{ab} would hit its maximum inside the 60° interval under discussion, in which case the functional form of e_{ab} would have to be set to the value of e_{ab} equal to $2nE_b$ at the appropriate place. With the present assumption it can be shown that the phase currents following commutation are:

$$
\begin{aligned}
i_a(\theta) &= i_a(\theta_c) \\
&\quad +\frac{E_b}{\Omega_b L}\left\{\frac{3}{\pi}\theta_c(\frac{1}{2}\theta_c-\theta_a)+\frac{3\theta_a}{\pi}\theta-\frac{3}{2\pi}\theta^2\right\} \\
&= \frac{E_b}{\Omega_b L}\left\{(\theta_a-\frac{\pi}{6})+\frac{3\theta_a}{\pi}\theta-\frac{3}{2\pi}\theta^2\right\} \\
i_b(\theta) &= -i_a(\theta) \\
i_c(\theta) &= 0 \\
&\quad \theta_c\le\theta\le\frac{\pi}{3}
\end{aligned}
\quad . \tag{16}
$$

The phase currents at the end of this interval are

$$
\begin{aligned}
i_a(\theta=\frac{\pi}{3}) &= \frac{E_b}{\Omega_b L}(2\theta_a-\frac{\pi}{3})\equiv -i_b(0) \\
i_b(\theta=\frac{\pi}{3}) &= -i_a(\frac{\pi}{3})\equiv -i_c(0) \\
i_c(\theta=\frac{\pi}{3}) &= 0\equiv i_a(0)
\end{aligned}
\quad , \tag{17}
$$

which confirms that the analysis of this single 60°-interval is sufficient to completely characterize the motor response. The

motor phase currents and the relevant back emf waveforms are shown in Fig. 4. The plot is for the example motor at a relative speed of four and an advance angle of 35°.

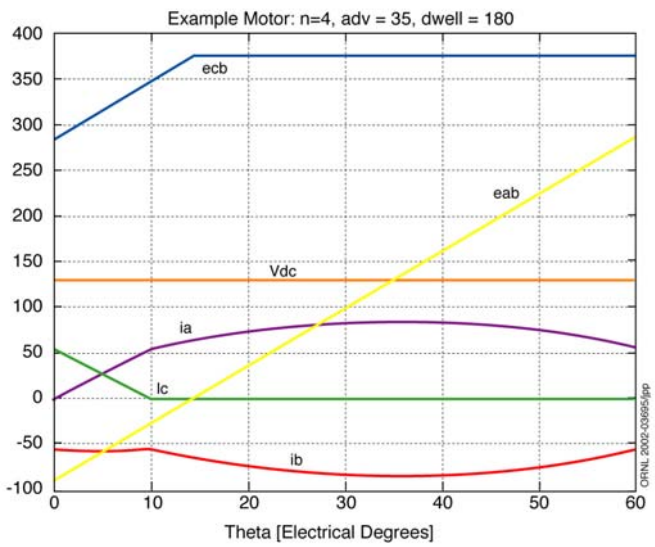

Fig. 4. Response of the analytical motor model in one 60° interval.

By interchanging the identities of the phases and recognizing that commutation occurs in both the positive and negative halves of the inverter the solutions above can be arranged to give the full solution for any of the phase currents over one cycle. For example to construct the phase a current during the positive half cycle, the a phase current above describes the first 60°; the negative of the phase b current above would describe the second 60° and the phase c current above would describe the last 60°.

The current waveforms in Eqs. (12) and (16) do not depend explicitly on the dc supply voltage, V_{dc}, or on the motor speed, n. The dependence on V_{dc} is implicit in the expressions because of the way that the advance angle is defined. If the dc supply voltage were to be lowered or raised so long as the advance angle remains fixed relative to the intersection of e_{ab} with the actual value of V_{dc}, the instantaneous currents will be the same. The dependence on motor speed is implicit in the rotor angle, θ, which is given by Eq. (6). Thus, the only impact of speed on the shape of the current waveforms is to compress them in time as the motor speed increases. For a fixed advance angle, θ_a, the shape of the phase currents over one fundamental cycle remains the same. Consequently, if the motor is capable of running within its rated current values and produces rated power at a low speed such as n = 2, it will be able to produce the same performance at any higher speed. The fact that the shape of the current waveform is dependent solely on the advance angle, which simply compresses or expands in time with motor speed, says that the CPSR for the BDCM is infinite when driven by the DMIC. In a practical drive the speed dependent losses, such as friction, windage, hysteresis, eddy current and winding resistance skin effect will limit the CPSR to a finite value. This analysis shows that the DMIC itself will not be a factor in limiting the CPSR.

The phase current solutions in Eqs. (12) and (17) can be used to compute the average power, and since the power has ripple of six times fundamental one can average over only the 60° interval under study. For a commanded dwell of 180° the dc link current is the sum of the incoming and outgoing phase currents and

$$\begin{aligned} P_{avg} &= \frac{3}{\pi}\int_0^{\pi/3} V_{dc}\ i_{dc}(\theta)\,d\theta \\ &= \frac{3}{\pi}\int_0^{\pi/3} V_{dc}\ \left[i_a(\theta)+i_c(\theta)\right]d\theta \\ &= \frac{3\ V_{dc}\ E_b}{\pi\ \Omega_b\ L}\left\{\frac{2}{3\pi}\theta_a^{\,3}+\frac{2}{3}\theta_a^{\,2}+\frac{2\pi}{9}\theta_a-\frac{4\pi^2}{81}\right\} \end{aligned} \quad . \tag{18}$$

This expression shows that the output power is linearly dependent on the supply voltage. If the supply voltage is reduced, increasing the advance angle may restore the desired power, but increasing the angle will also increase the magnitude of the motor current as shown below.

That portion of the total average output power that is associated with the outgoing phase is given by

$$\begin{aligned} P_c &= \frac{3}{\pi}\int_0^{\theta_c} V_{dc}\ i_c(\theta)\ d\theta \\ &= \frac{3\ V_{dc}\ E_b}{\pi\ \Omega_b\ L}\left[\frac{4}{3\ \pi}\ \theta_a^3+\frac{4}{3}\ \theta_a^2-\frac{5\ \pi}{9}\ \theta_a+\frac{4\ \pi^2}{81}\right] \end{aligned} \quad . \tag{19}$$

This power can be substantial and is the main reason why the power developed by the example motor at rated current is almost 48% higher at a relative speed of four as compared to base speed.

The peak current can also be obtained from the above expressions as an explicit function of the advance angle. The peak may occur in phase a or in phase b. When the peak in phase b is larger than the peak in phase a it means that the maximum current is experienced in the second 60° interval that the phase is energized. The peak current is given by:

$$\begin{aligned} I_{pk} &= \max\left\{i_a(\theta), -i_b(\theta)\right\} \\ &= \frac{E_b}{\Omega_b L} * \max\left\{\left[\frac{3\theta_a^{\,2}}{2\pi}+\theta_a-\frac{\pi}{6}\right],\left[\frac{2\theta_a^{\,2}}{\pi}+\frac{4\theta_a}{3}-\frac{5\pi}{18}\right]\right\} \end{aligned} \quad . \tag{20}$$

For advance angles less than 0.7666 radian (43.92°), the peak current is determined by the expression for phase a current and above this value, the current peaks in the second 60° interval and is determined by the phase b current expression.

The rms current can likewise be computed from the solutions for the phase currents in the single 60° interval analyzed above:

$$I_{rms} = \sqrt{\frac{1}{2\pi}\int_0^{2\pi} i_a(\theta)^2\, d\theta}$$

$$= \frac{E_b}{\Omega_b L}\left\{\sqrt{\frac{1}{\pi}\left[\begin{array}{l}\frac{8}{5\pi^2}\theta_a^{\,5} + \frac{8}{3\pi}\theta_a^{\,4} + \frac{16}{9}\theta_a^{\,3} \\ + \frac{4\pi}{27}\theta_a^{\,2} - \frac{16\pi^2}{81}\theta_a + \frac{23\pi^3}{1215}\end{array}\right]}\right\}. \qquad (21)$$

This theoretical analysis compares favorably to the results obtained with the simulator. For the example motor at n = 4, an advance angle of 49.68° and a 130 volt supply, the analytical expressions for the average power, peak current and rms current yield 29.66 kW, 240.3 amps and 174.7 amps respectively. These values compare favorably with the corresponding values shown in the simulation of Fig. 3, which are 29.69 kW, 204.3 amps and 174.3 amps respectively. The average power contributed by the outgoing phase is 9.91 kW per Eq. (19).

Now we consider the analysis for commanded transistor dwell of 120°.

4.2 Phase Currents with $\theta_d = 120°$

Consider again the transition from (c+,b-) to (a+,b-) but with 120° of commanded transistor dwell. In this case the outgoing phase (phase c) is de-energized by turning off transistor Q5, which transfers the phase c motor current from Q5 to the bypass diode D2. Thyristor, T5, conducts the phase c motor current until the current reaches zero at which time T5 shuts off. For this case, the commutation interval begins with

$$v_{ab} = +V_{dc},\ v_{cb} = 0. \qquad (22)$$

The initial phase currents are the same as for the 180° dwell case as given in Eq. (11).

The resulting phase currents during the commutation interval are:

$$\begin{aligned}
i_a(\theta) &= \frac{E_b}{\Omega_b L}\left\{\left[\frac{2\theta_a}{\pi} + \frac{2}{3} + \frac{V_{dc}}{3nE_b}\right]\theta - \frac{1}{\pi}\theta^2\right\} \\
i_b(\theta) &= \frac{E_b}{\Omega_b L}\left\{\left[\frac{\pi}{3} - 2\theta_a\right] + \left[-\frac{4\theta_a}{\pi} + \frac{2}{3} + \frac{V_{dc}}{3nE_b}\right]\theta + \frac{2}{\pi}\theta^2\right\} \\
i_c(\theta) &= \frac{E_b}{\Omega_b L}\left\{2\theta_a - \frac{\pi}{3} + \left[\frac{2\theta_a}{\pi} - \frac{4}{3} - \frac{2V_{dc}}{3nE_b}\right]\theta - \frac{1}{\pi}\theta^2\right\} \\
&0 \le \theta \le \theta_c
\end{aligned} \qquad (23)$$

where θ_c is the commutation angle. Comparing Eq. (12) with Eq. (23) we observe that the incoming phase current rises faster while the outgoing phase current phase current falls faster in the 120-degree dwell case as compared to the 180° case. Thus, the commutation period is shorter with 120-degree transistor dwell than with 180° of dwell. Also note that the currents in Eq. (23) depend explicitly on supply voltage and relative speed whereas the corresponding expressions in Eq. (12) do not.

Setting $i_c(\theta)$ in Eq. (23) to zero and solving for θ_c yields

$$\theta_c = \theta_a - \frac{2\pi}{3} - \frac{\pi V_{dc}}{3nE_b} + \sqrt{(\theta_a - \frac{2\pi}{3} - \frac{\pi V_{dc}}{3nE_b})^2 + \pi(2\theta_a - \frac{\pi}{3})}. \qquad (24)$$

The phase currents at the end of the commutation interval are

$$\begin{aligned}
i_a(\theta_c) &= \frac{E_b}{\Omega_b L}\left[(\frac{2\theta_a}{\pi} + \frac{2}{3} + \frac{V_{dc}}{3nE_b})\theta_c - \frac{1}{\pi}\theta_c^2\right] \\
i_b(\theta_c) &= -i_a(\theta_c) \\
i_c(\theta_c) &= 0
\end{aligned} \qquad (25)$$

After commutation is complete, the motor is running on only phases a and b and the model of Eq. (3) applies. The phase currents following commutation are:

$$\begin{aligned}
i_a(\theta) &= i_a(\theta_c) + \frac{E_b}{\Omega_b L}\left\{\frac{3}{\pi}\theta_c(\frac{1}{2}\theta_c - \theta_a) + \frac{3\theta_a}{\pi}\theta - \frac{3}{2\pi}\theta^2\right\} \\
i_b(\theta) &= -i_a(\theta) \\
i_c(\theta) &= 0. \\
\theta_c &\le \theta \le \frac{\pi}{3}
\end{aligned} \qquad (26)$$

The phase currents at the end of this interval are the same as those given in Eq. (17) and again we conclude that the analysis of this single 60° interval is sufficient to completely describe the motor operation over a full cycle.

The phase current solutions in Eqs. (23) and (26) can be used to compute the average power, and since the power has ripple of 6 times fundamental one can average over only the 60° interval under study. For the commanded dwell angle of 120° the dc supply current is the same as the incoming phase current over the entire interval

$$\begin{aligned}
P_{avg} &= \frac{3}{\pi}\int_0^{\pi/3} V_{dc}\ i_{dc}(\theta)\, d\theta \\
&= \frac{3}{\pi}\int_0^{\pi/3} V_{dc}\ i_a(\theta)\, d\theta \\
&= \frac{3V_{dc}E_b}{\pi\Omega_b L}\left\{\begin{array}{l}\frac{\pi}{6}\theta_a - \frac{\pi^2}{54} + (\frac{2\pi}{9} - \frac{1}{3}\theta_a + \frac{\pi V_{dc}}{9nE_b})\theta_c \\ + (\frac{-1}{6} + \frac{1}{2\pi}\theta_a - \frac{V_{dc}}{6nE_b})\theta_c^{\,2} - \frac{1}{3\pi}\theta_c^{\,3}\end{array}\right\}
\end{aligned} \qquad (27)$$

Because of the explicit dependence of the commutation angle and the phase currents on relative speed, n, and supply voltage, V_{dc}, the expressions for peak and rms current are not very compact. However, as the relative speed n grows progressively larger the motor current wave shapes for transistor dwell of 120° converge exactly to those given for the 180° case, i.e. Eqs. (23), (24), and (26) converge to the expressions in Eqs. (12), (13), and (16) respectively. Thus at very large n, the instantaneous, peak and

rms values of motor current are identical for either 120 or 180° of transistor dwell. However, the average power differs substantially. The limit of P_{avg} in Eq. (27) can be shown to be

$$P_{avg}(n \to \infty) = \frac{3V_{dc}E_b}{\pi\Omega_b L}\left[\frac{-2}{3\pi}\theta_a^{\,3} - \frac{2}{3}\theta_a^{\,2} + \frac{7\pi}{9}\theta_a - \frac{8\pi^2}{81}\right]. \qquad (29)$$

The above limit is the average power developed with a dwell angle of 180° as given by Eq. (18) minus the power contributed by the outgoing phase Eq. (19). Thus while the current wave forms at infinite speed are identical for the 120 and 180° dwell case, a dwell of 180° results in significantly more power.

A comparison of the commutation angle, peak current, rms current, and average power of the example motor operating at an advance angle of 49.68° for the 120° and 180° cases is displayed in Fig. 5. The relative speed is varied from 2 to a value of 25 in the figure. Note that the convergence of the 120° dwell performance to that of the 180° case is not rapid. At very high speed, the average power developed in the 120° dwell case is just about exactly the power rating of the motor at base speed (20.01 kW). For modest values of relative speed, and for a fixed advance angle, the 120° dwell results in a slightly lower peak and rms current and significantly less average power. Whether the dwell is 120 or 180° the DMIC still provides an infinite CPSR when all motor loss mechanisms are neglected.

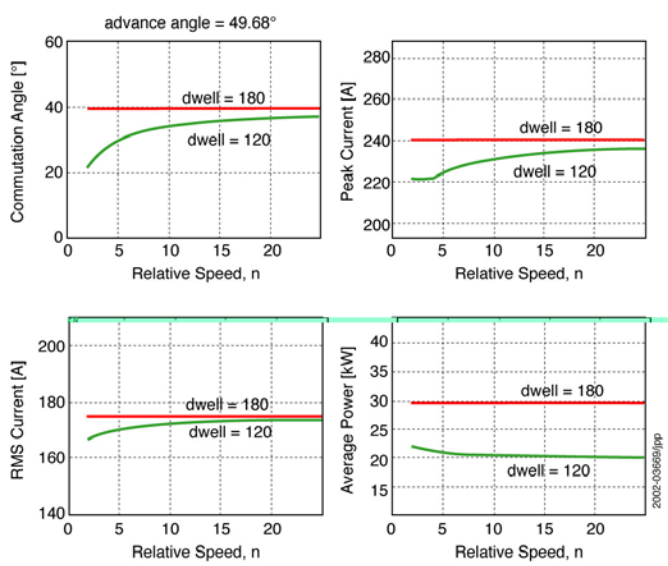

Fig. 5. The effect of dwell on commutation angle, rms and peak currents in phase a, and average power for the example motor with an advance angle of 49.7°.

4. Conclusions

The differential equations of the BDCM driven by the DMIC have been solved analytically for the case where all motor loss mechanisms are neglected. The analysis provides a theoretical verification that there is no inherent limit to the CPSR of a BDCM when driven by the DMIC. The analytic expressions developed for peak and rms current and average motor power, and specifically their dependence on motor inductance and dc supply voltage, will allow useful design guidance without simulation or laboratory experimentation.

References

1. J. S. Lawler et al. "Extending the Constant Power Speed Range of the Brushless DC Motor through Dual-Mode Inverter Control," IEEE Transactions on Power Electronics, submitted for review, August 2002.
2. J. M. Bailey et al., *Dual Mode Inverter Control Test Verification*, ORNL/TM-2000/172, Oak Ridge National Laboratory, UT-Battelle, LLC 2001.
3. J. M. Bailey and J. S. Lawler, *Constant Power Speed Range Extension of Surface Mounted PM Motors*, U.S. Patent Number 6,236,179 B1, Oak Ridge National Laboratory, UT-Battelle, LLC, May 22, 2001.
4. J. S. Lawler et al., *Extended Constant Power Speed Range of the Brushless DC Motor through Dual Mode Inverter Control*, ORNL/TM-2000/130, Oak Ridge National Laboratory, UT-Battelle, LLC 2001.
5. J. S. Lawler et al., "Limitations of the Conventional Phase Advance Method for Constant Power Operation of the Brushless DC Motor," IEEE SoutheastCon 2002, SEC-118, April 5-7, 2002.
6. Cambier et al., *Brushless DC Motor Using Phase Timing Advancement*, U.S. Patent Number 5,677,605, October 14, 1997.
7. J. M. Bailey, Principal Investigator, *Motor Models and Transient Analysis for High-Temperature, Superconductor Switch-Based Adjustable Speed Drive Applications*, TR-102338 3087-16, Electric Power Research Institute, June 1996.